Water Air Soil Pollut (2022) 233: 363
https://doi.org/10.1007/s11270-022-05776-6

Removal of Sodium Diclofenac from Aqueous Medium Using Layered Double Hydroxide: a Thermodynamic and Theoretical Approach

Carlos G. O. Bruziquesi · Farlon F. S. Xavier · Ingrid da S. Pacheco · Fábio A. do Amaral · Sheila C. Canobre · Mateus A. Gonçalves · Teodorico C. Ramalho · Liz M. Saavedra · Leandro V. A. Gurgel · Adilson C. Silva

Received: 21 December 2021 / Accepted: 13 July 2022 / Published online: 28 August 2022

Abstract In this study, an adsorbent based on layered double hydroxide (Co–Al–NO_3]-LDH) was synthesized by the co-precipitation method at constant pH 8.0±0.5. This new material was used for the removal of diclofenac from water. The X-ray diffraction pattern of [Co–Al–NO_3]-LDH revealed a basal spacing of 0.859 nm. Equilibrium time was reached after 120 min for an initial concentration (C_0) of diclofenac of 500 mg L^{-1}, and the pseudo-second order model best fitted the kinetic data obtained at C_0 values of 100, 250, and 500 mg L^{-1}. The isotherms performed at 15, 25, 35, and 45 °C showed an increase in the maximum adsorption capacity (Q_{max}=494.9 mg g^{-1}) up to 25 °C, but at temperatures above 25 ºC, the Q_{max} value was not increased. Equilibrium data were fitted using the Langmuir, Freundlich, and Sips models, and the change in standard free energy of adsorption was estimated from the Langmuir constant, corrected for the equilibrium activity coefficient, while the changes in standard enthalpy and entropy of adsorption were calculated from the van't Hoff equation. Adsorption studies as a function of nitrate concentration at two C_0 values (50 and 500 mg L^{-1}) showed that the increase in nitrate concentration led to a decrease in the Q_{max} of diclofenac, showing that nitrate competes with diclofenac for the adsorption sites. Theoretical studies were carried out using four different configurations of the diclofenac molecule approaching the surface of [Co–Al–NO_3]-LDH. The interaction distance between diclofenac and [Co–Al–NO_3]-LDH of 2.0 Å presented the lowest energy.

Keywords Layered double hydroxide · Diclofenac · Adsorption · Mechanism · Thermodynamics

Supplementary Information The online version contains supplementary material available at https://doi.org/10.1007/s11270-022-05776-6.

C. G. O. Bruziquesi · L. M. Saavedra · L. V. A. Gurgel · A. C. Silva (✉)
LQTA—Laboratório de Química Tecnológica e Ambiental, Departamento de Química, Instituto de Ciências Exatas e Biológicas, Universidade Federal de Ouro Preto, Campus Morro do Cruzeiro, Bauxita, Ouro Preto, Minas Gerais 35400-000, Brazil
e-mail: adilsoqui@ufop.edu.br; adilsonufla@gmail.com

F. F. S. Xavier · I. da S. Pacheco · F. A. do Amaral · S. C. Canobre
LAETE—Laboratório de Armazenamento de Energia e Tratamento de Efluentes, Instituto de Química, Universidade Federal de Uberlândia, Av. João Naves de Ávila, 2121, Campus Santa Mônica, Uberlândia, Minas Gerais 38408-100, Brazil

M. A. Gonçalves · T. C. Ramalho
Departamento de Química, Universidade Federal de Lavras, 37200-000 Lavras, Minas Gerais, Brazil

L. M. Saavedra
Fundación Universitaria de San Gil-UNISANGIL, Yopal, Casanare, Colombia

1 Introduction

Symptoms caused by strep throat, arthritis, and menstrual cramps are examples of pain and inflammation that can be defined as unpleasant sensations due to the stimulus associated with tissue damage, according to the medical community (Kantor, 1986; Vane, 1971). Diclofenac, marketed as Voltaren®, is widely used to treat pain (analgesic effect) and inflammatory diseases and also has anti-thermal action to control fever. Marketed for 40 years, approximately 50 mg of this drug may inhibit agents responsible for causing pain and inflammation (Dastidar et al., 2000), taking an average of 20 to 30 min to have a desirable effect.

However, despite its adverse side effects (Baigent et al., 2013), this pharmaceutical drug, excreted by humans as unchanged compounds or metabolites via urine, can cause damage to freshwater fish species (Schwaiger et al., 2004; Triebskorn et al., 2007; Yan et al., 2014). Other studies have demonstrated that diclofenac causes oxidative stress and reduces testosterone levels (Cherik et al., 2015). Concentrations of the order of μg L^{-1} and ng L^{-1} are a challenge for "conventional" water treatment methods, as water treatment plants cannot remove the entire portion of diclofenac, which is available in water at very low concentrations (Vogna et al., 2004).

Adsorption is a method applied to the treatment of water and wastewater. It is one of the cheapest and simplest purification and separation methods due to its versatility and accessibility, allowing the removal of hazardous compounds from water (Konicki et al., 2017; Qi et al., 2017; Xiong et al., 2017). Up to now, various materials, including magnetic oxides (Leone et al., 2018), mesoporous silica (Barczak et al., 2018), and even agricultural soils (Xu et al., 2009), were exploited as potential adsorbents for the treatment of water contaminated with diclofenac. Among these materials, carbonaceous materials (e.g. activated carbons) have been applied for the removal of pharmaceutical drugs from water. Some activated carbons have magnetic properties, which facilitate their separation process from water. Other activated carbons are capable of removing various pharmaceutical drugs, not depending on their ionic forms commonly detected in sewage. However, the magnetically activated carbons have disadvantages when their porosity decreases, which is the result of the introduction of Fe_3O_4 nanoparticles or other magnetic nanoparticles into their porous structures, or they have limited reuse (Rocha et al., 2020; Zhao et al., 2020).

The term "anionic clays" (AC) is used to represent LDHs (layered double hydroxides), natural or synthetic materials, which are obtained by the stacking of two-dimensional units called lamellae that are linked by intermolecular forces, such as London forces, electrostatic interaction, and hydrogen bonding (Li et al., 2017; Muráth et al., 2017; Yan et al., 2015). In these materials, species such as ions, atoms or molecules can be inserted into the interlamellar space through intercalation reactions (Sun & Dey, 2015). LDHs may contain divalent and trivalent metal cations simultaneously, with a generic formula $[M^{2+}_{1-x}M^{3+}_{x}(OH)_2[A^{n-}]_{x/n}ZH_2O_y]$, where M^{2+} can be Mg^{2+}, Zn^{2+}, or Co^{2+} and M^{3+} can be Al^{3+}, Ga^{3+}, Fe^{3+}, or Mn^{3+}. The term A^{n-} refers to a non-framework charge generally compensating for an inorganic anion (CO_3^{2-}, Cl^-, NO_3^-) and x is in the range of 0.2 to 0.4 (Evans & Slade, 2005; Khan & O'Hare, 2002; Wang & Ohare, 2012). LDHs have been applied to the synthesis of electrode materials for application in lithium batteries, magnetic hybrid materials, transport properties, and dye-sensitized solar cells (Wang & Ohare, 2012).

The process of adsorption using LDH materials for pollutant removal such as herbicides (Calisto et al., 2019; Lartey Young & Ma, 2022), fungicide and parasiticide (Roca Jalil et al., 2013), toxic metal ions (Feng et al., 2022), dyes (Yadav & Dasgupta, 2022), pharmaceuticals (Liu et al., 2022), and other substances that cause environmental damage has been reported in the literature. However, there are few studies involving the process of removing drugs from contaminated water using lamellar compounds. This study describes the synthesis of [Co–Al–NO_3]-LDH material by co-precipitation at constant pH (Calisto et al., 2019) and its application in the adsorption of diclofenac, an emerging pollutant, from aqueous solution. The thermodynamic parameters of adsorption were calculated, and the interaction between diclofenac and [Co–Al–NO_3]-LDH was elucidated by kinetic and theoretical studies.

2 Material and Methods

2.1 *Synthesis of [Co–Al–NO_3]-LDH*

[Co–Al–NO_3]-LDH was synthesized by the coprecipitation method at a constant pH. A volume of 500 mL of aqueous solutions containing Co^{2+} (1.0 mol L^{-1} of hexahydrate cobalt nitrate [$Co(NO_3)_2{\cdot}6H_2O$]) and Al^{3+} (0.5 mol L^{-1} of aluminum nitrate nonahydrate [$Al(NO_3)_3{\cdot}9H_2O$]), giving a metal ion ratio of 2:1, was slowly added to a solution with pH previously adjusted to 8.0 ± 0.5 by adding drops of an aqueous 1.0 mol L^{-1} NaOH solution. The powder obtained was filtered and dried under reduced pressure at 60–80 °C for 48 h.

2.2 *Structural and Morphological Characterizations of [Co–Al–NO_3]-LDH*

The structural characterization of [Co–Al–NO_3]-LDH was performed by X-ray diffraction (XRD) using a Shimadzu diffractometer (Model 6000, $Cu_{k\alpha}$ radiation, $\lambda = 1.5406$ Å), with a voltage of 40 kV, a current of 30 mA, and a scan speed of 2° min^{-1} from 5 to 70°. The unit cell parameters, *a*, *c*, and *d*, were calculated using the Full-Prof software. The d_{003} value corresponds to the sum of the thickness and height of the interlayer region.

Fourier transform infrared (FTIR) spectra of the solid samples were recorded from 500 to 4000 cm^{-1} on a Frontier single-range MIR spectrometer (Perkin Elmer), using the diamond attenuated total reflection (ATR) crystal accessory.

The morphological characterization of [Co–Al–NO_3]-LDH by scanning electron microscopy (SEM) coupled with energy-dispersive X-ray spectroscopy (EDS) was performed using a scanning electron microscope (Shimadzu, model SSX-550 SuperScan), operated with a filament voltage of 10 kV. The samples were supported on the sample holders to disperse the powder on conductive double-sided adhesive Scotch® tape. A 7-nm-thick gold layer was applied to the samples prior to measurements using a Bal-Tec sputter coater (model SCD 050).

The specific surface area and pore size distribution were determined by liquid N_2 adsorption at 77 K using the BET (Brunauer–Emmett–Teller) (Brunauer et al., 1938) and BJH (Barrett & Joyner, 1951) (Barrett–Joyner–Halenda) methods on Micrometrics ASAP® 2020 analyzer. Before measurements, samples were degassed under reduced pressure at 90 °C for 4 h.

The pH of the zero charge point (pH_{ZPC}) of the adsorbent was determined by the solid addition method (Hao et al., 2004). Samples of 20.0 mg of [Co–Al–NO_3]-LDH were placed into 50 mL Erlenmeyer flasks containing 20.0 mL of aqueous 0.1 mol L^{-1} NaCl solution. The initial pH ($pH_{initial}$) of the aqueous solutions was previously adjusted to different values, ranging from 2 to 12. Then, the flasks were agitated in an orbital shaker incubator at 180 rpm (Solab Scientific, model SL223) and 25 °C for 24 h to until the equilibrium pH was reached. After 24 h of agitation, the final pH (pH_{final}) of each flask was measured using a pH meter. The pH_{ZPC} was obtained by the intersection of the pH_{final} against $pH_{initial}$ curve with the abscissa, i.e., where the value of ΔpH is zero.

2.3 Adsorption Tests

2.3.1 Kinetic Studies

The kinetic adsorption studies of diclofenac were performed with 15.0 mg of [Co–Al–NO_3]-LDH dispersed in 15.0 mL of aqueous sodium diclofenac solution at initial concentrations (C_0) of 100, 250, and 500 mg L^{-1} and pH 7.0. Erlenmeyer flasks of 50 mL containing the dispersion were placed in an orbital shaker incubator (Solab Scientific, model Sl223) and agitated at 180 rpm and 25 ± 1 °C for different contact times. Aliquots of supernatants containing a residual concentration of diclofenac were taken and analyzed. The amount of diclofenac adsorbed on [Co–Al–NO_3]-LDH at a time *t* (Eq. (1)) was determined by measuring the concentration of diclofenac on a UV–VIS spectrophotometer (Hewlett–Packard, model 8453), at a wavelength of 275 nm. Previously, a standard calibration curve was prepared for the quantification of diclofenac in an aqueous solution (Online Resource 1).

$$q/(\mathrm{mg\,g^{-1}}) = \frac{(C_0 - C_t)V}{w} \quad (1)$$

where q (mg g^{-1}) is the adsorption capacity of [Co–Al–NO_3]-LDH, C_0 (mg L^{-1}) is the initial concentration of diclofenac, C_t (mg L^{-1}) is the

concentration of diclofenac at time t, V (L) is the volume of the diclofenac solution, and w (g) is the weight of [Co–Al–NO_3]-LDH. It is crucial to accurately describe the adsorption kinetics to determine the adsorption parameters by models that can predict the experimental behavior (Gerçel & Gerçel, 2007). For this, the following model equations frequently used to adjust the adsorption data in the aqueous phase were used: pseudo-first order (Lagergren, 1898), pseudo-second order (Ho & McKay, 1999), and intraparticle diffusion (Weber & Morris, 1963; Largitte & Pasquier, 2016). The integrated form of the pseudo-first order kinetic model is described in Eq. (2).

$$q_t/(\mathrm{mg g^{-1}}) = q_e\left[1 - e^{-k_1 t}\right] \tag{2}$$

where q_t (mg g^{-1}) is the amount of diclofenac adsorbed on [Co–Al–NO_3]-LDH at time t (min), q_e (mg g^{-1}) is the amount of diclofenac adsorbed on [Co–Al–NO_3]-LDH at equilibrium, and k_1 (min^{-1}) is the pseudo-first order rate constant. According to this model, the adsorption rate depends on the difference between the adsorbed amount at equilibrium and the adsorbed amount at time t. In other words, the adsorption rate decreases drastically when the amount adsorbed at time t is closer to the amount adsorbed at equilibrium. The initial adsorption rate (h) for the pseudo-first order kinetic model was calculated as described in Eq. (3).

$$h/(\mathrm{mg g^{-1} min^{-1}}) = k_1 q_e \tag{3}$$

The pseudo-second order kinetic model assumes that the adsorption capacity is proportional to the number of active sites located on the surface of the adsorbent, where k_2 (g mg^{-1} min^{-1}) is the pseudo-second order rate constant. The integrated form of the pseudo-second order model is described in Eq. (4).

$$q_t/(\mathrm{mg g^{-1}}) = \frac{q_e^2 k_2 t}{(1 + q_e k_2 t)} \tag{4}$$

The initial adsorption rate (h) for the pseudo-second order kinetic model was calculated as described in Eq. (5).

$$h/(\mathrm{mg g^{-1} min^{-1}}) = k_2 q_e^2 \tag{5}$$

The intraparticle diffusion (IPD) kinetic model (Eq. (6)) represents in detail that there may be one or more steps involved in the adsorption process. First, the adsorbate molecules approach the external surface of the solid (external diffusion) and then undergo diffusion through the thin film of solvent molecules surrounding the adsorbent particles. After, the adsorbate molecules undergo diffusion to the internal pores and the surface of the solid (intraparticle diffusion).

$$q_e/(\mathrm{mg g^{-1}}) = k_{it}^{0.5} + C \tag{6}$$

where k_{it} (mg g^{-1} $min^{-1/2}$) is the intraparticle diffusion rate constant and C is the intercept, which may be related to the thickness of the boundary layer.

2.3.2 Adsorption Isotherms

Adsorption equilibrium experiments were carried out at 15, 25, 35, and 45 °C, with agitation for 12 h at 180 rpm. Samples of 15.0 mL of aqueous diclofenac solution with initial concentrations ranging from 10 to 560 mg L^{-1} were added to 50 mL Erlenmeyer flasks. Subsequently, 15.0 mg of [Co–Al–NO_3]-LDH were added to each flask, and the flasks were agitated in an orbital shaker incubator (Tecnal, model TE-421) at 15, 25, 35, and 45 °C. When thermodynamic equilibrium was reached, the adsorbent was separated from the liquid phase by centrifugation. Equilibrium concentrations in the supernatants were determined on a UV–VIS spectrophotometer (Hewlett–Packard, model 8453) at a wavelength of 275 nm (Sect. 2.2.1).

Three isotherm models (Langmuir, Freundlich, and Sips) were used to fit the equilibrium adsorption data of diclofenac on [Co–Al–NO_3]-LDH. The Langmuir model (Langmuir, 1938) (Eq. (7)) assumes that the adsorption sites have equal energy (Ayawei et al., 2017). According to this model, the adsorption sites are finite, and there are no repulsive or attractive lateral interactions between the adsorbed species.

$$q_e/(\mathrm{mg g^{-1}}) = \frac{Q_{max} b C_e}{1 + b C_e} \tag{7}$$

where q_e (mg g^{-1}) corresponds to the amount of diclofenac adsorbed on [Co–Al–NO_3]-LDH at equilibrium, C_e (mg L^{-1}) is the equilibrium concentration of diclofenac in the liquid phase, Q_{max} (mg g^{-1}) corresponds to the maximum adsorption capacity of diclofenac on [Co–Al–NO_3]-LDH, and b (L mg^{-1}) corresponds to the Langmuir binding constant. Contrary to the Langmuir model, the Freundlich model (Freundlich, 1906) (Eq. (8)) assumes the occurrence

of multilayer adsorption onto the heterogeneous surface (Khayyun & Mseer, 2019).

$$q_e/(\mathrm{mg g^{-1}}) = k_F C_e^{1/n} \quad (8)$$

where k_F [(mg g^{-1})/(L mg^{-1})$^{1/n}$] is the Freundlich constant, which is related to the adsorption capacity of the adsorbent, and the term $1/n$ characterizes the adsorption intensity, indicating whether the adsorption is favorable ($1/n < 1$) or not ($1/n > 1$).

The last isotherm model, which is derived from the Langmuir and Freundlich model equations, is the Sips (Sips, 1948), or Langmuir–Freundlich model (Eq. (9)). If the value of the term n is greater than unity ($n > 1$), the adsorption system under study is considered heterogeneous. On the contrary, homogeneous adsorption is considered if the value of the term n is 1, and therefore the Sips model is reduced to the Langmuir model (Popoola, 2019).

$$q_e/\left(\mathrm{mg g^{-1}}\right) = \frac{Q_{max}\left(bC_e\right)^{1/n}}{\left(bC_e\right)^{1/n}} \quad (9)$$

2.3.3 Thermodynamic Calculations

The thermodynamic parameters (changes in standard enthalpy ($\Delta_{ads}H°$) and entropy ($\Delta_{ads}S°$) of adsorption) were estimated by the van't Hoff equation (Ghosal & Gupta, 2017), as described in Eq. (10).

$$lnK_a = \frac{-\Delta_{ads}H^{\circ}}{RT} + \frac{\Delta_{ads}S^{\circ}}{R} \quad (10)$$

where K_a (dimensionless) is the thermodynamic equilibrium constant, R (8.314 J K^{-1} mol^{-1}) is the gas constant, and T (K) is the absolute temperature.

The thermodynamic equilibrium constant can be estimated from the Langmuir binding constant, using the approach as suggested by the authors (Ghosal & Gupta, 2017; Liu, 2009) as described in Eq. (11).

$$K_a = \left[\frac{b}{\gamma_e}\left(1\mathrm{molL^{-1}}\right)\right] \quad (11)$$

where γ_e is the equilibrium activity coefficient (dimensionless), which was estimated using the value of the first equilibrium concentration of diclofenac from the plateau of the adsorption isotherms at different temperatures and applying it to Eq. (12).

$$\log\gamma_e = -0.5z^2\frac{\sqrt{\mu}}{1+\sqrt{\mu}} \quad (12)$$

where z corresponds to the ion charge in solution, i.e., -1 for diclofenac at pH 7.0, and μ (mol L^{-1}) is the ionic strength of the solution at equilibrium. The Guntelberg approximation of the extended Debye–Hückel law allows estimating ionic strengths up to 0.1 mol L^{-1} (Yokoyama & Yamatera, 1973).

The change in standard free energy of adsorption ($\Delta_{ads}G°$) was calculated by Eq. (13).

$$\Delta_{ads}G^{\circ}/(\mathrm{kJmol^{-1}}) = -\mathrm{RTlnK_a} \quad (13)$$

2.3.4 Effect of Nitrate Concentration on Adsorption Kinetics of Diclofenac on [Co–Al–NO_3]-LDH

The anion exchange properties of [Co–Al–NO_3]-LDH during adsorption of diclofenac were investigated. This experiment considered the hypothesis that the adsorption of diclofenac occurred with the release of nitrate from [Co–Al–NO_3]-LDH structure to the liquid phase and, therefore, the adsorption kinetics of diclofenac is affected by the presence of nitrate in solution. If this hypothesis is valid, the [Co–Al–NO_3]-LDH structure is probably modified after the adsorption of diclofenac. To investigate this hypothesis, 15.0 mg of [Co–Al–NO_3]-LDH was suspended in 50 mL Erlenmeyer flasks containing 15.0 mL of aqueous diclofenac solution at different initial concentrations (50 and 500 mg L^{-1}), and the flasks were agitated in an orbital shaker incubator at 180 rpm and 25 °C for different contact times, ranging from 15 to 180 min. The concentration of diclofenac in the liquid phase (supernatant) was determined as described in Sect. 2.2. The concentration of nitrate in the liquid phase was determined by UV–VIS spectrophotometry.

2.3.5 Theoretical Study: Optimization and Single Calculations

The construction of the geometries was performed in the Gauss View 5.0 software. After construction, optimization calculations of [Co–Al–NO_3]-LDH and diclofenac molecule were performed in the Gaussian 0.9 software with the functional PBE1PBE, and the basis set 6–311 g. Then, single-point calculations

were performed, approximating every 0.5 Å of the diclofenac molecule to the [Co–Al–NO_3]-LDH.

3 Results and Discussion

3.1 *Characterization of [Co–Al–NO_3]-LDH Before and After Adsorption of Diclofenac*

The anion exchange properties of [Co–Al–NO_3]-LDH were investigated by placing [Co–Al–NO_3]-LDH in contact with aqueous solutions of diclofenac at different initial concentrations, under the agitation of 180 rpm at 25 °C. Online Resource 2 shows curves of nitrate removal percentage against contact time in the presence of diclofenac (C_0 = 500 mg L^{-1}), under two different initial concentrations of nitrate (50 and 500 mg L^{-1}). Both curves showed similar behavior for nitrate removal from aqueous solution, i.e., the nitrate removal from solution did not depend on the initial concentration of diclofenac in the liquid phase. Online Resource 3 shows curves of adsorption capacity of diclofenac on [Co–Al–NO_3]-LDH as a function of contact time. The presence of nitrate in the solution negatively affected the adsorption of diclofenac on [Co–Al–NO_3]-LDH, decreasing its adsorption capacity (see kinetic data in Table 3). Figure 1 shows curves of diclofenac and nitrate concentration as a function of time. As can be seen in Fig. 1, as the concentration of diclofenac in solution decreases, the concentration of nitrate in solution increases, i.e., as diclofenac is adsorbed on [Co–Al–NO_3]-LDH, nitrate is released from [Co–Al–NO_3]-LDH structure. At 180 min of contact time, 18.7 mmol of diclofenac were adsorbed on [Co–Al–NO_3]-LDH while 20.5 mmol of nitrate were released from [Co–Al–NO_3]-LDH structure, giving a nitrate-to-diclofenac ratio of 1.1. Therefore, the stoichiometry of the reaction (Eq. (14)) was close to 1. These data confirmed that diclofenac was adsorbed on [Co–Al–NO_3]-LDH by anion exchange, as the presence of nitrate affected the adsorption capacity of diclofenac, probably inhibiting the displacement of nitrate ions from [Co–Al–NO_3]-LDH structure to solution and the migration of diclofenac from the bulk solution to the surface of [Co–Al–NO_3]-LDH. This phenomenon can also be observed in the X-ray diffractograms (Fig. 2) and FTIR spectra (Fig. 3) of [Co–Al–NO_3]-LDH before and after adsorption of diclofenac. X-ray diffractograms of [Co–Al–NO_3]-LDH before and after adsorption of diclofenac are shown in Fig. 2, which shows the crystalline structure of [Co–Al–NO_3]-LDH was clearly modified as the amount of adsorbed diclofenac increased. Basal distances and unit cell parameters for [Co–Al–NO_3]-LDH materials before and after adsorption of diclofenac are shown in Table 1. The X-ray diffractograms of the synthesized

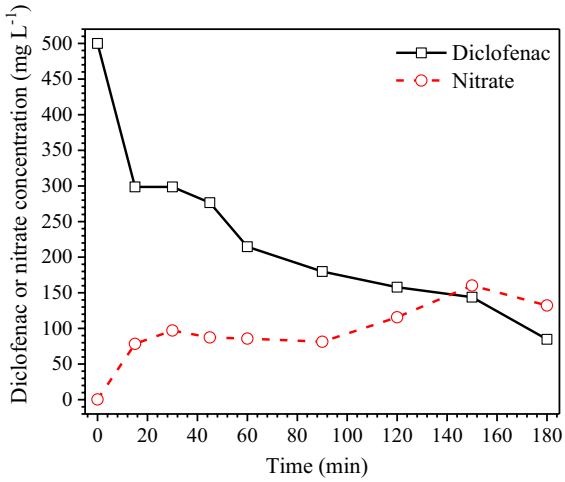

Fig. 1 Evolution of diclofenac and nitrate concentration during adsorption of diclofenac (C_0 = 500 mg L^{-1}) on [Co–Al–NO_3]-LDH at 25 °C

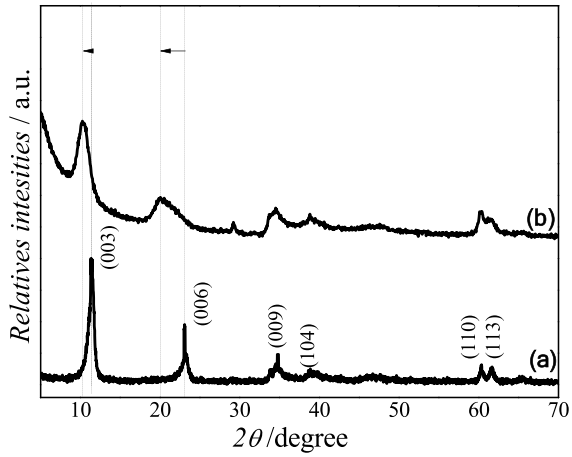

Fig. 2 X-ray diffractograms of **a** [Co–Al–NO_3]-LDH before adsorption of diclofenac and **b** [Co–Al–NO_3]-LDH after adsorption of diclofenac

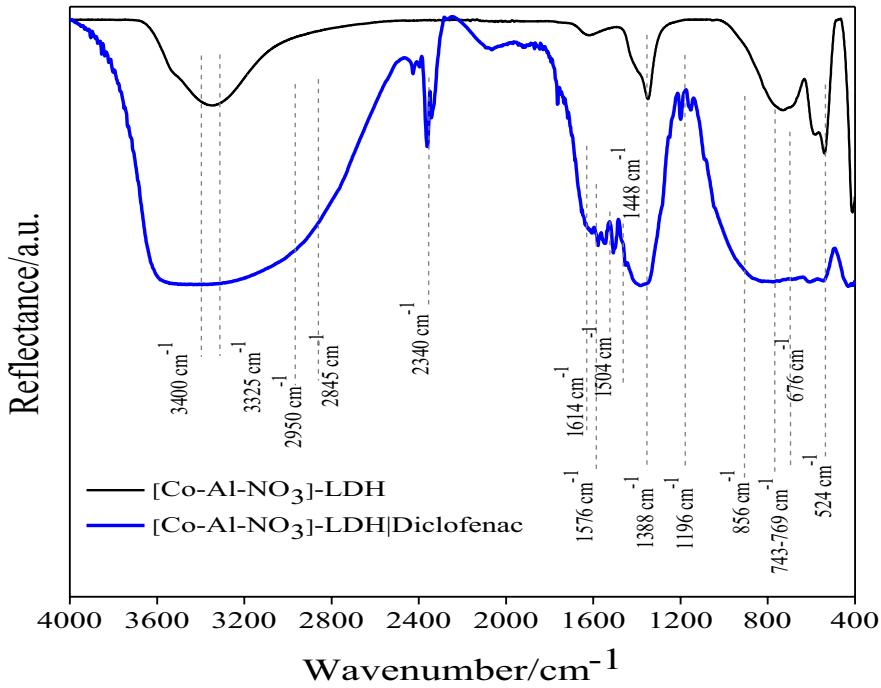

Fig. 3 FTIR spectra of [Co–Al–NO_3]-LDH before and after adsorption of diclofenac. Experimental conditions: 15.0 mg of [Co–Al–NO_3]-LDH, 15.0 mL of diclofenac (500 mg L^{-1}), and time of 12 h, under agitation of 150 rpm at 25 °C

Table 1 Unit cell parameters of [Co–Al–NO_3]-LDH before and after adsorption of diclofenac

Sample	d_{003} / Å	a^* / Å	c^{**} / Å	V^{***} / Å^3	Representation of the unit cell
Hydrotalcite (JCPDS 14-191)	7.74	3.07	23.23	189.60	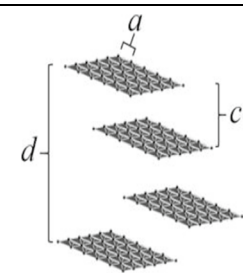
[Co-Al-NO_3]-LDH after adsorption	8.59	3.06	25.76	208.57	
[Co-Al-NO_3] LDH before adsorption	8.02	3.10	24.07	200.31	

(*) $a = 2 \times d_{110}$; (**) $c = 3 \times d_{003}$; (***)V = volume = $\frac{\sqrt{3}a^2c}{2} = 0.866a^2c$

[Co–Al–NO_3]-LDH showed sharp diffraction peaks, as can be seen in Fig. 2. The basal (003) reflections represent the thickness of the layer in hydrotalcite-like materials. As shown in Fig. 2, the X-ray diffractogram of [Co–Al–NO_3]-LDH showed typical characteristic reflections of the two-dimensional hydrotalcite phase and were indexed according to JCPDS Card No. 14–191, which showed basal planes (003), (006), (009), (110), and (113) at 2θ of 10.14, 20.04, 34.70, 60.43, and 61.80º, respectively (Millange et al., 2000). These data confirm that the proposed synthesis method was useful to obtain a crystalline [Co–Al–NO_3]-LDH material.

$$\text{LDH} - NO_3 + \text{diclofenac}^- \rightarrow \text{LDH} - \text{diclofenac} + NO_3^- \quad (14)$$

The basal spacing d_{003}, which represents the thickness of the hydrotalcite layer plus the interlayer space, is a function of the size and orientation of the intercalated anions. The basal spacing of the

[Co–Al–NO_3]-LDH was calculated using Bragg's law ($2\theta = 10.14°$, $d_{003} = 0.859$ nm). Table 1 shows unit cell parameters of hydrotalcite (JCPDS card no. 14–191) and [Co–Al–NO_3]-LDH before and after adsorption of diclofenac. As can be seen in Table 1, a change in the unit cell parameters was observed after adsorption of diclofenac, suggesting the exchange of nitrate for diclofenac in the [Co–Al–NO_3]-LDH structure. This change in the basal planes (003) and (006) is related to an increase in the value of the interlamellar distance d_{003}, due to the intercalation of the diclofenac molecule in the interlayer structure of [Co–Al–NO_3]-LDH. It was also observed that the value of d_{003} increased after adsorption of diclofenac from 8.02 to 8.59 Å and, consequently, there was also an increase in the unit cell volume from 200.31 to 208.57 Å.

FTIR spectroscopy was used to clarify the interaction of diclofenac with [Co–Al–NO_3]-LDH. The FTIR spectra before and after adsorption of diclofenac on [Co–Al–NO_3]-LDH is shown in Fig. 3. The bands at 524 and 676 cm^{-1} are related to vibrations of Co–O and Al–O bonds in [Co–Al–NO_3]-LDH (Chen et al., 2011). In addition, the bands at 1635, 1651, and 3400 cm^{-1} correspond to the stretching vibration of the water molecule (O–H bond) in [Co–Al–NO_3]-LDH due to the presence of water of hydration and hydroxyl groups in the [Co–Al–NO_3]-LDH structure.

The characteristic bands of the functional groups present in diclofenac and [Co–Al–NO_3]-LDH were identified in the FTIR spectrum of [Co–Al–NO_3]-LDH after adsorption of diclofenac ($C_0 = 500$ mg L^{-1}) (Fig. 3). In this spectrum, a broadening of the bands at 3400 and 3325 cm^{-1} was observed. These bands correspond to the stretching vibration of the O–H and N–H groups (Chu et al., 2012), respectively. The wag vibration of the N–H bond was observed at 856 cm^{-1}, which was attributed to the secondary amine group in diclofenac. Vibrations of other functional groups identified in the spectrum of [Co–Al–NO_3]-LDH after adsorption of diclofenac were: C–H bond at 856, 2845, and 2950 cm^{-1} (Chu et al., 2012), C–Cl bond at 743–769 cm^{-1}, and C=C bond in the aromatic ring at 1504 cm^{-1} (Ramachandran & Ramukutty, 2014). The bands at 1576 and 1448 cm^{-1} correspond to asymmetric and symmetric stretching vibrations of the carboxylate ion, respectively (Venugopal et al., 2007). The spectrum of [Co–Al–NO_3]-LDH after adsorption of diclofenac suggested a possible interaction due to the adsorption of diclofenac molecule on [Co–Al–NO_3]-LDH, which is related to the widening and deformation of the bands related to the Co–O bond at 524 cm^{-1} and Al–O bond at 676 cm^{-1}.

In an adsorption process, the adsorbate molecules migrate from the bulk solution to the pores and surface of the adsorbent. However, the adsorption of ionizable adsorbate molecules depends directly on the charge of active sites on the surface of the adsorbent. The point of zero charge is defined as the pH value where the net surface charge of the adsorbent is zero. Figure 4 shows a plot of pH_{final} against $pH_{initial}$ used for estimating the pH_{ZPC} value ($pH_{ZPC} = 7.92$). Therefore, at pH lower than pH_{ZPC}, [Co–Al–NO_3]-LDH has a net positive surface charge, whereas at pH higher than pH_{ZPC}, it has a net negative surface charge. As the ZPC value of [Co–Al–NO_3]-LDH is higher than 7 and the pK_a value of the diclofenac molecule is 4.15 (see Online Resource 4), it is expected that the adsorption of diclofenac molecules on [Co–Al–NO_3]-LDH is favored at pH 7 (Wishart et al., 2008). Therefore, at pH values lower than pH_{ZPC}, the net surface charge of the [Co–Al–NO_3]-LDH is positive, which makes the adsorption of negatively charged diclofenac molecules favorable. In this study, all the adsorption experiments were performed at pH 7.0, considering that river water has a pH close to neutrality.

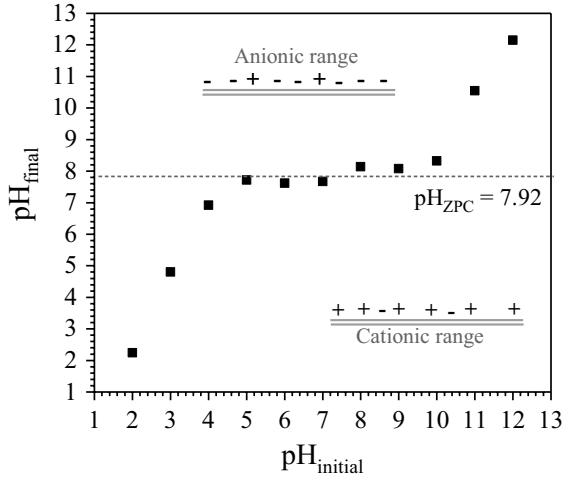

Fig. 4 Plot of pH_{final} versus $pH_{initial}$ used to obtain the point of zero charge of the [Co–Al–NO_3]-LDH adsorbent

The analysis of the textural properties of the adsorbent material aimed to evaluate the presence of micropores, mesopores, and macropores in its structure. This makes it possible to determine the characteristics related to the porosity and specific surface area of the synthesized material that affect the performance of the [Co–Al–NO_3]-LDH adsorbent for the removal of diclofenac from the aqueous phase (Rouquerol et al., 2013; Marsh & Rodríguez-Reinoso, 2006). Figure 5 shows the adsorption and desorption isotherms of N_2 for [Co–Al–NO_3]-LDH, which is a type II isotherm (Thommes et al., 2015). As can be seen in Fig. 5, the adsorption of N_2 on [Co–Al–NO_3]-LDH at low relative pressures (P/P_0) suggests the presence of micropores. In addition, when the value of P/P_0 approached unity, the isotherm curve increased sharply due to the presence of macropores in the sample. The phenomenon of hysteresis in the isotherm curve in the range of P/P_0 from 0.5 to 0.9 revealed the presence of mesopores. Using the P/P_0 range proposed by the BET method (linear range), the specific surface area and pore volume of [Co–Al–NO_3]-LDH were determined.

Table 2 shows the textural properties determined for [Co–Al–NO_3]-LDH by the BET method (specific surface area) and BJH method (pore size distribution). The specific surface area of [Co–Al–NO_3]-LDH was 34 m^2g^{-1}, with a great development in the number of mesopores with an average size of 123 Å and a volume of 1.7 cm^3g^{-1}, providing more active sites on the surface of the adsorbent for the removal of diclofenac.

Figure 6 shows SEM/EDS images of [Co–Al–NO_3]-LDH. These images showed irregular plate-like structures overlapped forming layers as if they were non-uniformly stacked lamellae, which are typically found in hydrotalcite structures (Gregg and Sing, 1982). EDS microanalysis of [Co–Al–NO_3]-LDH revealed amounts of Co^{2+} and Al^{3+} of 33.65 and 7.89%, respectively, indicating the presence of these cations in the [Co–Al–NO_3]-LDH structure.

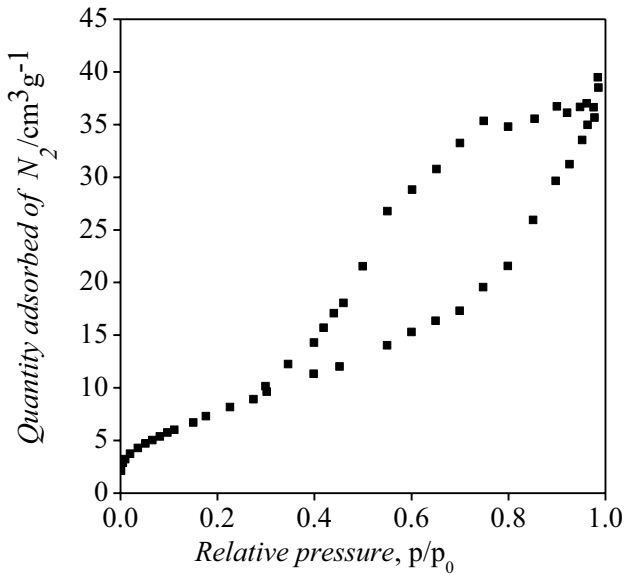

Fig. 5 Physisorption isotherms (adsorption/desorption) of N_2 on [Co–Al–NO_3]-LDH

Table 2 Textural properties of [Co–Al–NO_3]-LDH

Material	Specific surface area (m^2g^{-1})	Average pore diameter (Å)		Average pore volume (cm^3g^{-1})		
		Micro	Meso	Micro	Meso	Total
[Co–Al–NO_3]-LDH	34	-	123	0.02	1.7	1.7

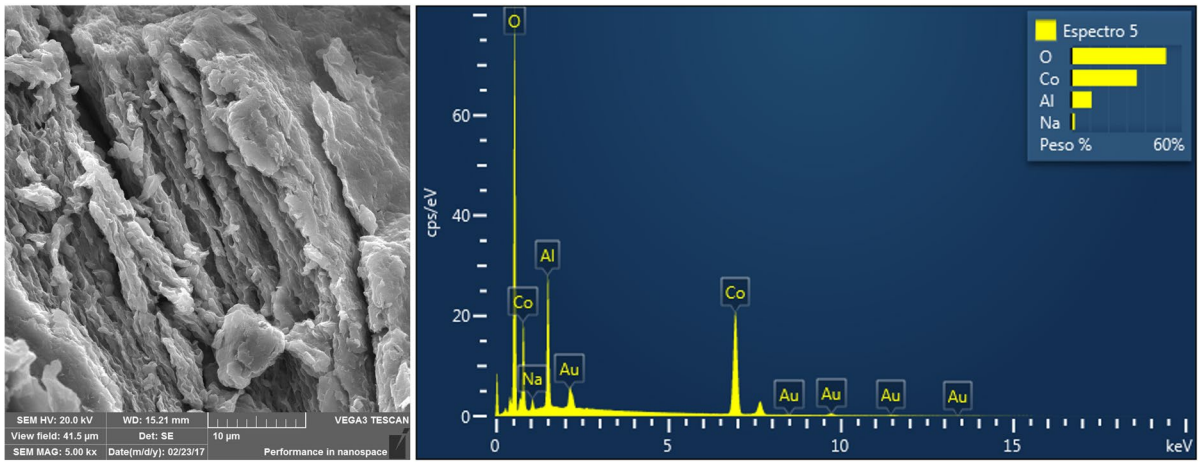

Fig. 6 SEM/EDS images of [Co–Al–NO_3]-LDH

3.2 Adsorption Tests

3.2.1 Kinetic Studies

The evolution of the adsorption capacity of [Co–Al–NO_3]-LDH for diclofenac was studied at three initial concentrations of diclofenac (100, 250, and 500 mg L^{-1}) to estimate the effect of the initial concentration of diclofenac on kinetic parameters, such as equilibrium adsorption capacity (q_e) and adsorption rate constant (k), as well as clarify the mechanism of adsorption. The evolution of the adsorption capacity of [Co–Al–NO_3]-LDH for diclofenac at three initial concentrations as a function of contact time is shown in Fig. 7.

Three adsorption kinetic models (pseudo-first and pseudo-second order and intraparticle diffusion) were used to model the kinetic data. The kinetic parameters estimated by these models are important to elucidate the mechanism of adsorption of diclofenac on [Co–Al–NO_3]-LDH. For the pseudo-first and pseudo-second order, the curves fitted to the experimental data are shown in Fig. 7a, while the straight lines fitted to the experimental data by the intraparticle diffusion model are shown in Fig. 7b. Table 3 shows the kinetic parameters estimated by fitting the pseudo-first- and pseudo-second order models to the experimental data. Table 4 shows the kinetic parameters estimated by fitting the intraparticle diffusion model to the experimental data.

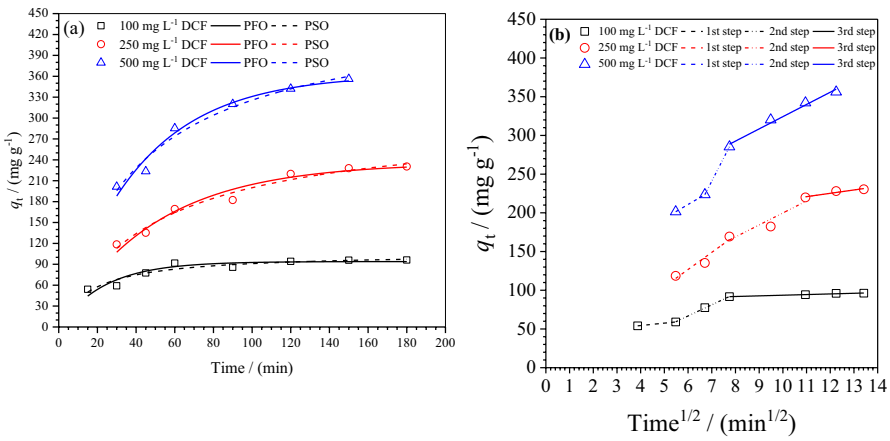

Fig. 7 **a** Adsorption capacity (q_t) of diclofenac (DCF) on [Co–Al–NO_3]-LDH as a function of time (t) at different initial concentrations of diclofenac (100, 250, and 500 mg L^{-1}) at 25 °C, with the pseudo-first and pseudo-second order curves fitted to the experimental data and **b** intraparticle diffusion plots for the adsorption of diclofenac on [Co–Al–NO_3]-LDH

Table 3 Kinetic parameters estimated by the pseudo-first and pseudo-second order models for adsorption of diclofenac (DCF) on [Co–Al–NO_3]-LDH at 25 °C

$C_{0,DCF}$/(mg L^{-1})		Pseudo-first order					
		$q_{e,est}$/(mg g^{-1})	k_1/(min^{-1})	h/(mg g^{-1} min^{-1})	R^2_{adj}	χ^2_{red}	*RSS*
100		93.95 ± 3.36	(4.26 ± 0.63) × 10^{-2}	4.00	0.8514	42.08	252.11
250		235.69 ± 8.20	(2.03 ± 0.20) × 10^{-2}	4.78	0.9564	89.02	445.09
500		362.73 ± 11.15	(2.44 ± 0.22) × 10^{-2}	8.83	0.9654	140.37	561.47
$C_{0,DCF}$/(mg L^{-1})	$C_{0,NO3}^-$/(mg L^{-1})	$q_{e,est}$/(mg g^{-1})	k_1/(min^{-1})	h/(mg g^{-1} min^{-1})	R^2_{adj}	χ^2_{red}	*RSS*
500	50	262.67 ± 7.23	(2.04 ± 0.15) × 10^{-2}	5.36	0.9919	38.58	154.30
500	500	319.26 ± 12.31	(1.47 ± 0.13) × 10^{-2}	4.68	0.9875	97.03	485.16
$C_{0,DCF}$/(mg L^{-1})		Pseudo-second order					
		$q_{e,est}$/(mg g^{-1})	k_2/(g mg^{-1} min^{-1})	h/(mg g^{-1} min^{-1})	R^2_{adj}	χ^2_{red}	*RSS*
100		106.38 ± 4.92	(5.57 ± 1.42) × 10^{-4}	6.30	0.8878	31.72	190.31
250		297.92 ± 14.20	(6.86 ± 1.26) × 10^{-5}	6.08	0.9686	64.10	320.52
500		455.36 ± 22.25	(5.52 ± 1.06) × 10^{-5}	11.44	0.9674	132.18	528.72
$C_{0,DCF}$/(mg L^{-1})	$C_{0,NO3}^-$/(mg L^{-1})	$q_{e,est}$/(mg g^{-1})	k_2/(g mg^{-1} min^{-1})	h/(mg g^{-1} min^{-1})	R^2_{adj}	χ^2_{red}	*RSS*
500	50	349.11 ± 22.04	(5.21 ± 1.16) × 10^{-5}	6.35	0.9835	78.77	315.07
500	500	438.06 ± 19.24	(2.77 ± 0.39) × 10^{-5}	5.32	0.9929	55.02	275.10

Table 4 Kinetic parameters estimated by the intraparticle diffusion model for adsorption of diclofenac (DCF) on [Co–Al–NO_3]-LDH at 25 °C

$C_{0,DCF}$ /(mg L^{-1})		$k_{it,1}$ (mg g^{-1} $min^{-1/2}$)	$k_{it,2}$	$k_{it,3}$	$C_{i,1}$ (mg g^{-1})	$C_{i,2}$	$C_{i,3}$	$R_{i,1,adj}^2$	$R_{i,2,adj}^2$	$R_{i,3,adj}^2$
100		3.09	14.41	0.83	42.12	− 19.64	85.31	1	0.9986	0.9598
250		22.11	15.49	4.33	− 5.86	44.93	173.32	0.8835	0.7971	0.8518
500		17.96	59.60	15.79	103.03	− 176.29	166.33	1	1	0.9752
$C_{0,DCF}$/(mg L^{-1})	$C_{0,NO3}^-$/(mg L^{-1})	$k_{it,1}$ (mg g^{-1} $min^{-1/2}$)	$k_{it,2}$	$k_{it,3}$	$C_{i,1}$ (mg g^{-1})	$C_{i,2}$	$C_{i,3}$	$R_{i,1,adj}^2$	$R_{i,2,adj}^2$	$R_{i,3,adj}^2$
500	50	28.80	8.87	-	− 41.92	141.01	-	0.9713	0.9944	-
500	500	29.13	22.38	-	− 41.43	6.96	-	0.9558	0.9987	-

As can be seen in Fig. 7a, as the diclofenac concentration increases, the equilibrium adsorption capacity was reached more slowly, i.e., in 40 min for C_0 of 100 mg L^{-1}, 120 min for C_0 of 250 mg L^{-1}, and more than 120 min for C_0 of 500 mg L^{-1}. The pseudo-second order model fitted the experimental data better than the pseudo-first order model, as can be seen by the values of R^2_{adj}, χ^2_{red}, and *RSS*. As can be seen in Fig. 7b, the adsorption of diclofenac on [Co–Al–NO_3]-LDH occurred in two or more steps. First, there was a slower initial adsorption step, followed by a faster adsorption step and a slower adsorption step. At lower concentrations of diclofenac (100 and 250 mg L^{-1}), the value of $k_{i,2}$ was very similar. The slower adsorption rates ($k_{i,2}$ and $k_{i,3}$) of diclofenac at lower concentrations suggest that the adsorption of diclofenac occurred mainly on the surface of [Co–Al–NO_3]-LDH, because the lower concentration of diclofenac, the lower the driving force for adsorption of diclofenac in the pores of [Co–Al–NO_3]-LDH. As the initial concentration of diclofenac increased to 500 mg L^{-1}, the mechanism of adsorption seems to have changed, with the $k_{i,2}$ and $k_{i,3}$ values for the C_0 value of 500 mg L^{-1} much higher than the $k_{i,2}$ and $k_{i,3}$ values for the C_0 values of 100 and 250 mg L^{-1}.

The effect of the presence of nitrate at two different concentrations (50 and 500 mg L^{-1}) on the adsorption kinetics of diclofenac (C_0 = 500 mg L^{-1}) on [Co–Al–NO_3]-LDH was also investigated. The kinetic parameters estimated by fitting the

pseudo-first and pseudo-second order models and intraparticle diffusion model to the experimental data are shown in Tables 3 and 4, respectively. As can be seen in Tables 3 and 4, the presence of nitrate in an aqueous solution negatively affected the adsorption kinetics of diclofenac, decreasing the equilibrium adsorption capacity and adsorption rate constant for adsorption of diclofenac on [Co–Al–NO_3]-LDH. These results confirm that diclofenac is adsorbed on [Co–Al–NO_3]-LDH by anion exchange.

3.2.2 *Adsorption Isotherms and Adsorption Thermodynamics*

The adsorption isotherms were carried out at 15 °C (288,15 K), 25 °C (298,15 K), 35 °C (308,15 K), and 45 °C (318.15 K), with an equilibrium time of 160 min and an agitation speed of 180 rpm. The isotherm models used to model the equilibrium data were Langmuir, Freundlich, and Sips. The plots of equilibrium adsorption capacity (q_e) against equilibrium concentration (C_e) are shown in Fig. 8. The parameters estimated by fitting the isotherm models to the equilibrium data are shown in Table 5. The highest adsorption capacity (Q_{max} = 494.9 mg g^{-1}) of [Co–Al–NO_3]-LDH for diclofenac was observed at 25 °C (298.15 K). The best fits according to the R^2_{adj}, χ^2_{adj}, and *RMSE* values were provided by the Sips model for the isotherms obtained at 15 (288.15 K) and 25 °C (298.15 K) and the Langmuir model for the adsorption isotherms obtained at 35 (308.15 K) and 45 °C (318.15 K). However, the Q_{max} values predicted by the Sips model for the adsorption isotherms obtained at 15 (288.15 K) and 25 °C (298.15 K) are not in agreement with the $q_{e,exp}$ values (experimental equilibrium adsorption capacity). On the other hand, the Q_{max} values predicted by the Langmuir model for the adsorption isotherms obtained at 15 (288.15 K) and 25 °C (298.15 K) are in good agreement with

Table 5 Isotherm model parameters estimated by the Langmuir, Freundlich, and Sips models for adsorption of diclofenac on [Co–Al–NO_3]-LDH at different temperatures

Model	Parameter	Temperature (K)			
		288.15	298.15	308.15	318.15
	$q_{e,exp}$ (mg g^{-1})	443.9	494.9	482.8	475.1
Freundlich	k_F (mg g^{-1})(L g^{-1})$^{1/n}$	143.7	127.2	181.8	179.6
	n	3.49	2.68	3.60	3.79
	χ^2_{red}	1090.5	1511.3	3885.7	5327.7
	R^2_{adj}	0.952	0.953	0.873	0.807
	R^2	0.978	0.977	0.939	0.903
	RMSE	33.02	38.88	62.34	72.99
Langmuir	Q_{max} (mg g^{-1})	497.9	548.5	504.9	482.8
	b (L mg^{-1})	0.134	0.186	0.418	0.521
	χ^2_{red}	1722.2	705.5	231.8	574.8
	R^2_{adj}	0.938	0.978	0.993	0.980
	R^2	0.972	0.989	0.995	0.991
	RMSE	41.50	26.55	15.22	23.98
Sips	Q_{max} (mg g^{-1})	772.1	620.6	508.7	849.1
	b (L mg^{-1})	0.033	0.129	0.485	0.022
	n	1.96	1.25	1.05	2.18
	χ^2_{red}	976.4	613.0	659.2	946.5
	R^2_{adj}	0.965	0.981	0.978	0.962
	R^2	0.986	0.991	0.991	0.985
	RMSE	31.25	24.76	25.68	30.76

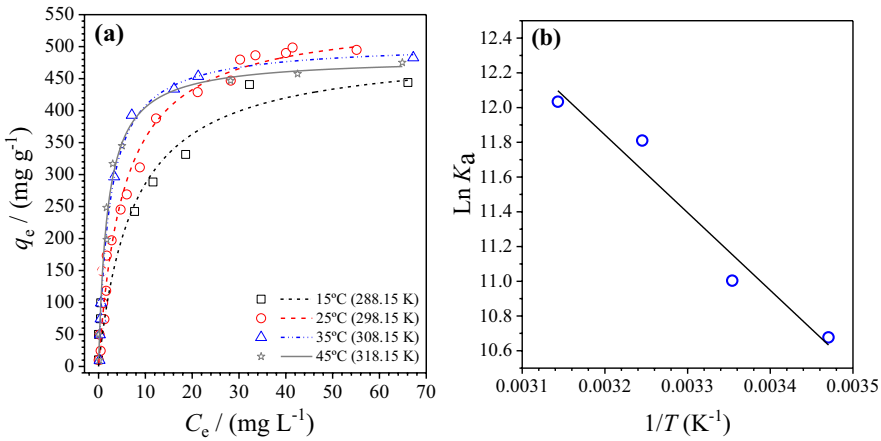

Fig. 8 **a** Adsorption isotherms of diclofenac on [Co–Al–NO_3]-LDH at pH 7.0 and 15 °C (288.15 K), 25 °C (298.15 K), 35 °C (308.15 K), and 45 °C (318.15 K). **b** van't Hoff plot for adsorption of diclofenac on the [Co–Al–NO_3]-LDH adsorbent at pH 7.0

the $q_{e,exp}$ values. Therefore, the isotherm model that best described the adsorption of diclofenac on [Co–Al–NO_3]-LDH was the Langmuir model.

The Sips model is based on the Freundlich and Langmuir models. This model assumes that at low equilibrium concentrations, the adsorption is described by the Freundlich isotherm and at high equilibrium concentrations by the Langmuir isotherm (Istratie et al., 2016). In addition, the Sips model assumes that the adsorption occurs at heterogenous sites on the surface of the adsorbent containing different energies (Damjanovic et al., 2010). The heterogeneity of the adsorption system under study is described by the parameter *n*. For homogeneous adsorption the value of *n* is equal to 1 and the Sips isotherm is reduced to the expression of the Langmuir isotherm, whereas for values of *n* different from unity, heterogeneous adsorption, is assumed (Zhang et al., 2012). The values of the parameter *n* for the adsorption isotherms of diclofenac obtained at different temperatures were greater than 1, indicating that the adsorption systems under study are heterogeneous (Damjanovic et al., 2010; Foo & Hameed, 2010). In fact, [Co–Al–NO_3]-LDH is an adsorbent material with a heterogeneous surface and probably with adsorption sites with different energy contents.

The Langmuir model assumes that the adsorption occurs in monolayer on a surface with finite and equal energy content adsorption sites. This model also assumes uniform adsorption at active sites with no lateral interaction and no migration of adsorbed species to neighboring adsorption sites (Bakr et al., 2018). Based on these assumptions, the adsorption of diclofenac on [Co–Al–NO_3]-LDH did not occur as predicted by the Langmuir model, although the Langmuir model was able to mathematically describe the adsorption systems under study at different temperatures (Zhang et al., 2021).

The value of parameter *b* is related to the affinity of binding sites on the surface of [Co–Al–NO_3]-LDH for diclofenac molecules. The higher the value of parameter *b*, the higher the affinity of [Co–Al–NO_3]-LDH for diclofenac molecules (Jorge Gonçalves et al., 2021). The value of parameter *b* was 0.418 L mg^{-1} (133.0 L $mmol^{-1}$) at 35 °C (308.15 K) and 0.521 (165.8) L mg^{-1} at 45 °C (318.15 K), which is in agreement with the steeper slope of the adsorption isotherms as temperature was increased, indicating higher affinity of active sites on [Co–Al–NO_3]-LDH for diclofenac molecules as temperature was increased.

Table 6 shows the thermodynamic parameters estimated by the van't Hoff equation ($\Delta_{ads}H^{o}$ and ($\Delta_{ads}S^{o}$) and the approach suggested by Liu, (2009) ($\Delta_{ads}G^{o}$). The thermodynamic parameters, changes in standard free energy ($\Delta_{ads}G^{o}$), enthalpy ($\Delta_{ads}H^{o}$), and entropy ($\Delta_{ads}S^{o}$) of adsorption are useful to understand the adsorption process of diclofenac on [Co–Al–NO_3]-LDH.

The $\Delta_{ads}G^{\circ}$ values were negative for all adsorption systems under study, with more negative $\Delta_{ads}G^{\circ}$ values as the temperature increased representing the closest equilibrium position to the products ([Co–Al–NO_3]-LDH-DCF) (Liu et al., 2013; Martínez et al., 2018). Adsorption processes can be classified as physical or chemical according to the $\Delta_{ads}H^{o}$ value. If the $\Delta_{ads}H^{o}$ value is lower than 80 kJ mol^{-1}, the phenomenon that governs the adsorption is physisorption, but if the $\Delta_{ads}H^{o}$ value is in the range of 80–400 kJ mol^{-1}, the phenomenon that governs adsorption is chemisorption (Martínez et al., 2017). The $\Delta_{ads}H^{\circ}$ value estimated for adsorption of diclofenac on [Co–Al–NO_3]-LDH was 37.19 kJ mol^{-1}, which indicates a phenomenon governed by physisorption, probably due to the formation of electrostatic interactions between adsorption sites on the surface of [Co–Al–NO_3]-LDH and diclofenac molecules. In addition, the adsorption of diclofenac on [Co–Al–NO_3]-LDH was endothermic. The entropic term, $T\Delta_{ads}S^{\circ}$, was positive, which indicates an increase in the degrees of freedom for the species involved in the adsorption process, i.e. water molecules involved in the hydration of active sites were released from [Co–Al–NO_3]-LDH to bulk solution and nitrate ions were released from [Co–Al–NO_3]-LDH to bulk solution, while diclofenac molecules migrated from the bulk solution to the surface of [Co–Al–NO_3]-LDH. For an adsorption process to be

Table 6 Thermodynamic parameters for adsorption of diclofenac on [Co–Al–NO_3]-LDH at pH 7.0

Thermodynamic parameter	Temperature/*K*			
	288.15	298.15	308.15	318.15
$\Delta_{ads}G^{\circ}$/(kJ mol^{-1})	−25.47	−27.65	−29.82	−32.00
$\Delta_{ads}H^{\circ}$/(kJ mol^{-1})		37.19		
$T\Delta_{ads}S^{\circ}$/(kJ mol^{-1})		64.84		

spontaneous, the following condition must be met: $\Delta_{ads}G° = \Delta_{ads}H – T\Delta_{ads}S° < 0$ (Martínez et al., 2018). As the adsorption process under study was endothermic, to meet this condition, the process must involve an entropy gain. As the entropic term was higher than the enthalpic term, the adsorption system under study was entropically driven.

3.2.3 *Theoretical Study: Optimization, Single Calculations, and Potential Energy Curve*

Theoretical studies play an important role in the study of material surfaces at the molecular level (Mesquita et al., 2016). Four arrangement possibilities (MP1, MP2, MP3, and MP4) of the diclofenac molecule to adsorb on the surface of [Co–Al–NO_3]-LDH were investigated and are shown in Fig. 9. The evolution of energy related to the type of orientation (parallel or perpendicular) and the interaction distance of the different chemical groups of the diclofenac molecule with the surface of [Co–Al–NO_3]-LDH (MP1, MP2, MP3, and MP4) was evaluated every 0.5 Å. The results obtained are shown in Fig. 10. As can be seen in Fig. 10, it was observed that the MP1 configuration

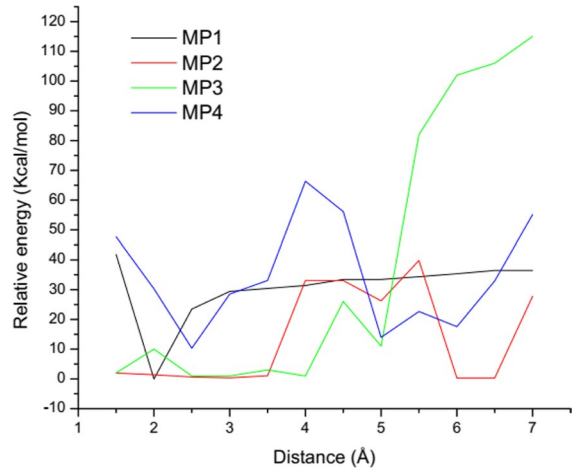

Fig. 10 Evolution of the relative energy with the interaction distance of the diclofenac molecule and the surface of [Co–Al–NO_3]-LDH

with an interaction distance of 2.0 Å presented lower energy in relation to the other configurations investigated (MP2, MP3, and MP4).

It is also important to note that the MP2 configuration with an interaction distance of 2.5 Å

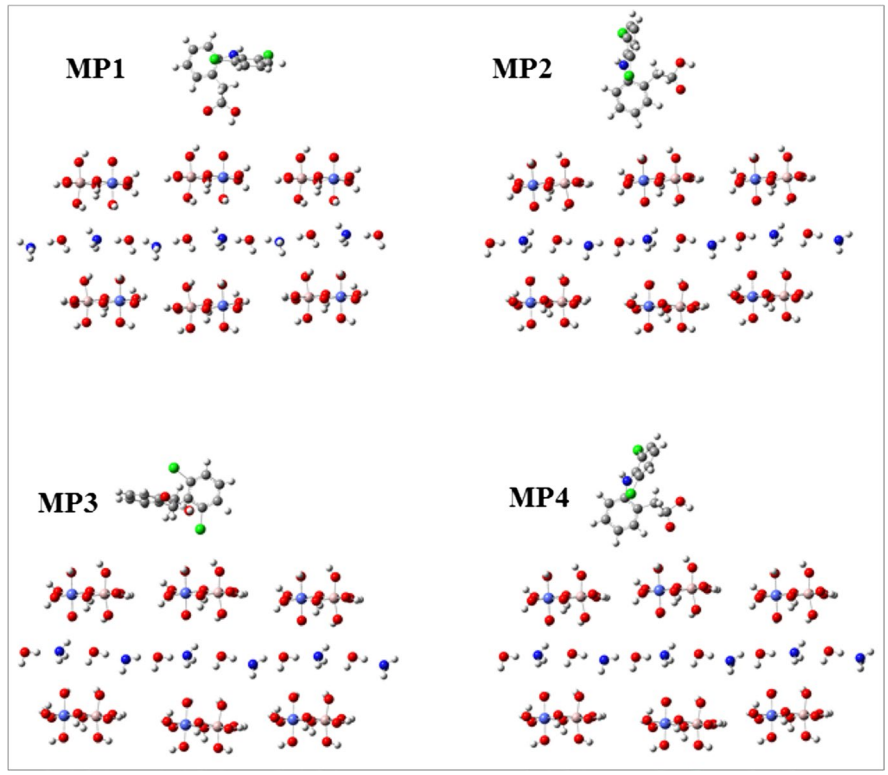

Fig. 9 Schematic view of diclofenac molecule interacting with the surface of [Co–Al–NO_3]-LDH in four different arrangements: MP1 (the functional group of diclofenac interacts perpendicularly with the surface of [Co–Al–NO_3]-LDH); MP2 (the functional group of diclofenac interacts parallelly with the surface of [Co–Al–NO_3]-LDH); MP3 (the functional group of diclofenac interacts parallelly with the surface of [Co–Al–NO_3]-LDH); MP4 (the functional group of diclofenac interacts perpendicularly with the surface of [Co–Al–NO_3]-LDH)

presented an energy value very close to the MP1 configuration and, in fact, these two configurations (MP1 and MP2) were more promising due to the formation of the frontal hydrogen bonding between the diclofenac molecule and the surface of [Co–Al–NO_3]-LDH. This shows that adsorption occurred preferentially in the MP1 configuration, i.e., a configuration of lower energy. The MP3 configuration presented relative energy greater than the MP1 and MP2 configurations. In this configuration, the diclofenac molecule approached the surface of [Co–Al–NO_3]-LDH by the chlorine atom. Thus, the formation of a halogen bonding between the chlorine atom and the hydrogen atom on the surface of [Co–Al–NO_3]-LDH was observed. In fact, the energy of the MP3 configuration is expected to be higher as the hydrogen bonding is stronger than the halogen bonding. In the MP4 configuration, much higher energy was observed in relation to the other configurations, and, therefore, the adsorption probably did not occur in this configuration. As can be seen in Fig. 10, the MP1 configuration with an interaction distance of 2.0 Å had the lowest energy, and this configuration is the way in which the adsorption of the diclofenac molecule on the surface of [Co–Al–NO_3]-LDH probably occurred. The hydrogen bonding contributed significantly to the stabilization of the system. Theoretical calculation using the spin density distribution was useful to understand the influence of hydrogen bonding on the stability of this configuration. The results obtained from this calculation are shown in Fig. 11.

The spin density distribution in a given paramagnetic molecule indicates the contributions due to electrons with the majority spin (α) and the minority spin (β) (Alarcón et al., 2010; Patinec et al., 2013). In general, α-spin density represents from where electrons are coming, while the β-spin density represents to where the electrons are going. In Fig. 11, these regions are represented by the colors blue (spin α) and green (spin β). In this figure, it is possible to observe a high spin density around the surface of [Co–Al–NO_3]-LDH, mainly spin α. This indicates that electrons are leaving the diclofenac molecule and arriving at the surface of [Co–Al–NO_3]-LDH, providing high stability to the system.

4 Conclusions

This study presented the synthesis of a promising adsorbent material ([Co–Al–NO_3]-LDH) with a simple and low-cost synthesis method for use in the removal of diclofenac from water. [Co–Al–NO_3]-LDH showed a specific surface area of 34 m^2g^{-1}, great development of the number of mesopores with an average size of 123 Å, and pH of zero charge point of 7.92. The basal spacing of [Co–Al–NO_3]-LDH was calculated using the Bragg's law ($2\theta = 10.14°$, $d_{003} = 0.859$ nm). After adsorption of diclofenac, the concentration of nitrate in aqueous solution increased and the basal spacing of [Co–Al–NO_3]-LDH also increased, suggesting that ion exchange may have occurred. The adsorption mechanism of diclofenac

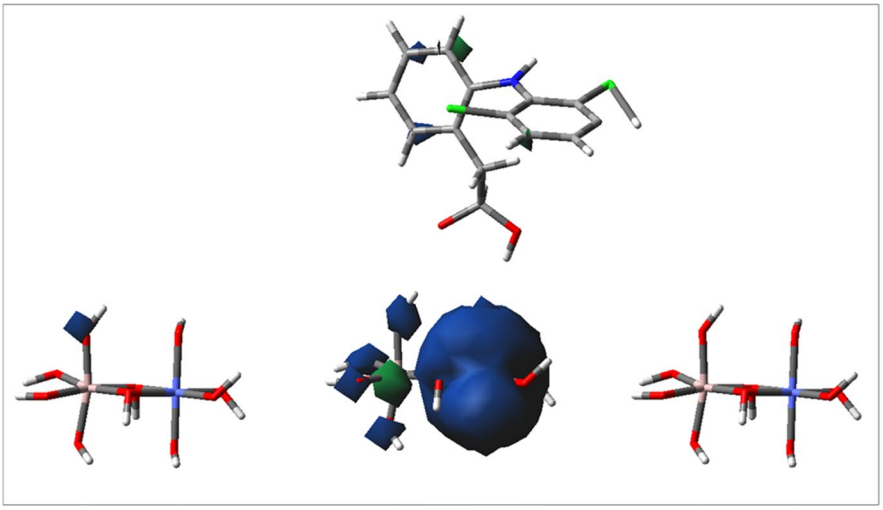

Fig. 11 Spin-density map of the MP1 configuration with an interaction distance of 2.0 Å (the isosurface contour value is 0.0004)

on [Co–Al–NO_3]-LDH presented three steps and was affected by the presence of nitrate in aqueous solution, confirming that anion exchange was involved in the adsorption of diclofenac on [Co–Al–NO_3]-LDH. The adsorption isotherms were better fitted by the Langmuir model. The highest equilibrium adsorption capacity was 494.9 mg g^{-1} at 25 °C. The $\Delta_{ads}H°$ value (37.19 kJ mol^{-1}) indicated a phenomenon of physisorption of diclofenac on [Co–Al–NO_3]-LDH, which is probably related to the formation of electrostatic interactions between diclofenac and [Co–Al–NO_3]-LDH. In addition, the value of the entropic term ($T\Delta_{ads}S°$) (64.84 kJ mol^{-1}) indicated an increase in the degrees of freedom of the system after adsorption and that the adsorption process was entropically driven. From the theoretical studies, the MP1 configuration with an interaction distance between the diclofenac molecule and the surface of [Co–Al–NO_3]-LDH of 2.0 Å presented the lowest energy, showing that this configuration is the most likely configuration for adsorption of diclofenac on [Co–Al–NO_3]-LDH.

Acknowledgements The authors are grateful to the Federal University of Ouro Preto (UFOP grant number 23109.003209/2016-98), the Federal University of Uberlandia (UFU), the National Council for Scientific and Technological Development (CNPq grant number 443426/2014-7), the Minas Gerais State Research Funding Foundation (FAPEMIG grant numbers APQ-00847-14, PQ-02249-14, and APQ-03219-14), and the National Council for the Improvement of Higher Education (CAPES, Finance Code 001) for funding this research. The authors thank Dr. Liliane C. Soares (UFOP) for providing the speciation curve for diclofenac.

Author Contribution Farlon F. S. Xavier, Ingrid da S. Pacheco, Fábio A. do Amaral, and Sheila C. Canobre: These authors were responsible for the synthesis and some characterizations of the material. Mateus A. Gonçalves and Teodorico de C. Ramalho: These authors were responsible for the theoretical calculations that helped to understand how adsorption occurs. Liz M. Saavedra and Carlos G. O. Bruziquesi: These authors were responsible for the kinetic, equilibrium, and thermodynamic adsorption tests. Leandro V. A. Gurgel and Adilson C. Silva: These authors were responsible for modeling the kinetic and thermodynamic adsorption data, conference the entire text, and analysis of some characterizations.

Funding The Minas Gerais State Research Funding Foundation (FAPEMIG grant numbers APQ-03226–18, APQ-00847–14, APQ-02249–14, and APQ-03219–14), the National Council for Scientific and Technological Development (CNPq grant number 443426/2014–7), and the National Council for the Improvement of Higher Education (CAPES, Finance Code 001).

Data Availability Not applicable.

Declarations

Ethics Approval Not applicable.

Consent to Participate Not applicable.

Consent for Publication Not applicable.

Competing Interests The authors declare no competing interests.

References

Alarcón, E., González-Béjar, M., Gorelsky, S., et al. (2010). Photophysical characterization of atorvastatin (Lipitor®) ortho-hydroxy metabolite: Role of hydroxyl group on the drug photochemistry. *Photochemical & Photobiological Sciences*. https://doi.org/10.1039/c0pp00102c

Ayawei, N., Ebelegi, A. N., Wankasi, D. (2017). Modelling and interpretation of adsorption isotherms. *Journal of Chemistry*. https://doi.org/10.1155/2017/3039817

Baigent, C., Bhala, N., Emberson, J., et al. (2013). Vascular and upper gastrointestinal effects of non-steroidal anti-inflammatory drugs: Meta-analyses of individual participant data from randomised trials. *Lancet, 382*, 769–779. https://doi.org/10.1016/S0140-6736(13)60900-9

Bakr, A. A., Sayed, N. A., Salama, T. M., et al. (2018). Kinetics and thermodynamics of Mn(II) removal from aqueous solutions onto Mg-Zn-Al LDH/montmorillonite nanocomposite. *Egyptian Journal of Petroleum, 27*, 1215–1220. https://doi.org/10.1016/j.ejpe.2018.05.003

Barczak, M., Wierzbicka, M., & Borowski, P. (2018). Sorption of diclofenac onto functionalized mesoporous silicas: Experimental and theoretical investigations. *Microporous and Mesoporous Materials*. https://doi.org/10.1016/j.micromeso.2018.01.013

Barrett, E. P., Joyner, L.G., & Halenda, P. P. (1951). The determination of pore volume and area distributions in porous substances. I. Computations from nitrogen isotherms. *Journal of the American Chemical Society, 73*(1), 373–380.

Brunauer, S., Emmett, P. H., & Teller, E. (1938). Adsorption of gases in multimolecular layers. *Journal of the American Chemical Society, 60*, 309–319. https://doi.org/10.1021/ja01269a023

Calisto, J. S., Pacheco, I. S., Freitas, L. L., et al. (2019). Adsorption kinetic and thermodynamic studies of the 2, 4 – dichlorophenoxyacetate (2,4-D) by the [Co–Al–Cl] layered double hydroxide. *Heliyon, 5*, e02553. https://doi.org/10.1016/j.heliyon.2019.e02553

Chen, C., Qu, J., Cao, C., et al. (2011). CuO nanoclusters coated with mesoporous SiO2 as highly active and

stable catalysts for olefin epoxidation. *Journal of Materials Chemistry*. https://doi.org/10.1039/c0jm04568c

Cherik, D., Benali, M., Louhab, K. (2015). Occurrence, ecotoxicology, removal of diclofenac by adsorption on activated carbon and biodegradation and its effect on bacterial community: A review. *World Science News, 10,* 116–144.

Chu, C.-C., White, K. L., Liu, P., et al. (2012). Electrical conductivity and thermal stability of polypropylene containing well-dispersed multi-walled carbon nanotubes disentangled with exfoliated nanoplatelets. *Carbon N Y, 50*, 4711–4721. https://doi.org/10.1016/J.CARBON.2012.05.063

Damjanovic, L., Rakic, V., Rac, V., et al. (2010). The investigation of phenol removal from aqueous solutions by zeolites as solid adsorbents. *Journal of Hazardous Materials, 184*, 477–484.

Dastidar, S. G., Ganguly, K., Chaudhuri, K., & Chakrabarty, A. N. (2000). The anti-bacterial action of diclofenac shown by inhibition of DNA synthesis. *International Journal of Antimicrobial Agents*. https://doi.org/10.1016/S0924-8579(99)00159-4

Evans, D. G., & Slade, R. C. T. (2005). Structural aspects of layered double hydroxides. *Structure and Bonding*. https://doi.org/10.1007/430_005

Feng, X., Long, R., Wang, L., Liu, C., Bai, Z., & Liu, X. (2022). A review on heavy metal ions adsorption from water by layered double hydroxide and its composites. *Separation and Purification Technology., 284*, 120099. https://doi.org/10.1016/j.seppur.2021.120099

Foo, K. Y., & Hameed, B. H. (2010). Insights into the modeling of adsorption isotherm systems. *Chemical Engineering Journal, 156*, 2–10. https://doi.org/10.1016/j.cej.2009.09.013

Freundlich, H. M. F. (1906). Over the adsorption in solution. *Journal of Physical Chemistry, 57*, 385–471. https://doi.org/10.1159/000090887

Gerçel, Ö., & Gerçel, H. F. (2007). Adsorption of lead(II) ions from aqueous solutions by activated carbon prepared from biomass plant material of Euphorbia rigida. *Chemical Engineering Journal*. https://doi.org/10.1016/j.cej.2007.01.010

Ghosal, P. S., & Gupta, A. K. (2017). Determination of thermodynamic parameters from Langmuir isotherm constant-revisited. *Journal of Molecular Liquids*. https://doi.org/10.1016/j.molliq.2016.11.058

Gregg, S. J., & Sing, K. S. W. (1982). Adsorption, surface area and porosity (2nd ed.). Academic Press, New York.

Hao, X., Quach, L., Korah, J., et al. (2004). The control of platinum impregnation by PZC alteration of oxides and carbon. *Journal of Molecular Catalysis a: Chemical*. https://doi.org/10.1016/j.molcata.2004.04.026

Ho, Y. S., & McKay, G. (1999). Pseudo-second order model for sorption processes. *Process Biochemistry, 34*, 451–465. https://doi.org/10.1016/S0032-9592(98)00112-5

Istratie, R., Stoia, M., Păcurariu, C., Locovei, C. (2016). Single and simultaneous adsorption of methyl orange and phenol onto magnetic iron oxide/carbon nanocomposites. *Arabian Journal of Chemistry. 12*(8), 3704–3722. https://doi.org/10.1016/j.arabjc.2015.12.012

Gonçalves, F. J., Gurgel, L. V. A., Soares, L. C., Teodoro, F. S., Ferreira, G. M. D., Coelho, Y. L., da Silva, L.H.M.,Prim, D., & Gil, L. F. (2021). Application of pyridine-modified chitosan derivative for simultaneous adsorption of Cu(II) and oxyanions of Cr(VI) from aqueous solution. *Journal of Environmental Management*, *282,* 111939. https://doi.org/10.1016/j.jenvman.2021.111939

Kantor, T. G. (1986). Use of diclofenac in analgesia. *American Journal of Medicine*. https://doi.org/10.1016/0002-9343(86)90083-5

Khan, A. L., O'Hare, D. (2002). Intercalation chemistry of layered double hydroxides: Recent developments and applications. *Journal of Materials Chemistry, 12*(11), 3191–3198. https://doi.org/10.1039/B204076J

Khayyun, T. S., & Mseer, A. H. (2019). Comparison of the experimental results with the Langmuir and Freundlich models for copper removal on limestone adsorbent. *Applied Water Science*. https://doi.org/10.1007/s13201-019-1061-2

Konicki, W., Aleksandrzak, M., Moszyński, D., & Mijowska, E. (2017). Adsorption of anionic azo-dyes from aqueous solutions onto graphene oxide: Equilibrium, kinetic and thermodynamic studies. *Journal of Colloid and Interface Science, 496*, 188–200. https://doi.org/10.1016/j.jcis.2017.02.031

Lagergren, S. Y. (1898). Zur theorie der sogenannten adsorption gelöster stoffe, kungliga svenska vetenskapsakademiens. *Handlingar, 24*, 1–39.

Langmuir, I. (1938). The adsorption of gases on plane surfaces of glass, mica and platinum. *Journal of the American Chemical Society, 60*, 467–475. https://doi.org/10.1021/ja01269a066

Largitte, L., & Pasquier, R. (2016). A review of the kinetics adsorption models and their application to the adsorption of lead by an activated carbon. *Chemical Engineering Research and Design, 109*, 495–504. https://doi.org/10.1016/j.cherd.2016.02.006

Lartey Young, G., & Ma, L. (2022). Optimization, equilibrium, adsorption behaviour of Cu/Zn/Fe LDH and LDHBC composites towards atrazine reclamation in an aqueous environment. *Chemosphere, 133526*, 2022. https://doi.org/10.1016/j.chemosphere.2022.133526

Leone, V. O., Pereira, M. C., Aquino, S. F., et al. (2018). Adsorption of diclofenac on a magnetic adsorbent based on maghemite: Experimental and theoretical studies. *New Journal of Chemistry*. https://doi.org/10.1039/c7nj03214e

Li, H., Li, J., Xu, C., et al. (2017). Hierarchically porous MoS2/CoAl-LDH/HCF with synergistic adsorption-photocatalytic performance under visible light irradiation. *Journal of Alloys and Compounds*. https://doi.org/10.1016/j.jallcom.2016.12.310

Liu, K., Zhu, B., Feng, Q., Wang, Q., Duan, T., Ou, L., ... & Lu, Y. (2013). Adsorption of Cu(II) ions from aqueous solutions on modified chrysotile: Thermodynamic and kinetic studies. *Applied Clay Science, 80*, 38–45. https://doi.org/10.1016/j.clay.2013.05.014

Liu, X., Yang, S., Feng, T., Zhong, H., Cao, S., & Chen, Y. (2022). Removal of amoxicillin from water by concrete-based hydrotalcites: Efficiency and mechanism. *Process*

Safety and Environmental Protection., 163, 210–217. https://doi.org/10.1016/j.psep.2022.04.063

Liu, Y. (2009). Is the free energy change of adsorption correctly calculated ? 1981–1985

Marsh, H., & Rodríguez-Reinoso, F. (2006). Activated Carbon (1st ed.). Madrid: Elsevier Ltd, pp 143–242.

Martínez, L. N., Baeta, B. E. L., Pereira, M. C., et al. (2017). Thermodinamic study of a magnetic molecular imprinted polymer for removal of nitrogenous pollutant from gasoline. *Fuel, 210*, 380–389. https://doi.org/10.1016/j.fuel.2017.08.087

Martínez, L., Penido, R. G., De Azevedo, S. L., et al. (2018). Molecularly imprinted polymers for selective adsorption of quinoline: Theoretical and experimental studies. *RSC Advances, 8*, 28775–28786. https://doi.org/10.1039/c8ra04261f

Mesquita, A. M., Guimarães, I. R., de Castro, G. M. M., et al. (2016). Boron as a promoter in the goethite (α-FeOOH) phase: Organic compound degradation by Fenton reaction. *Applied Catalysis b: Environmental*. https://doi.org/10.1016/j.apcatb.2016.03.051

Millange, F., Walton, R. I., & O'Hare, D. (2000). Time-resolved in situ X-ray diffraction study of the liquid-phase reconstructitm of Mg-Al-carboaate hydrotalcite-like compounds. *Journal of Materials Chemistry, 10*, 1713–1720. https://doi.org/10.1039/b002827o

Muráth, S., Dudás, C., Kukovecz, Á., et al. (2017). From nicotinate-containing layered double hydroxides (LDHs) to NAD coenzyme–LDH nanocomposites – syntheses and structural characterization by various spectroscopic methods. *Journal of Molecular Structure, 1140*, 39–45. https://doi.org/10.1016/j.molstruc.2016.11.083

Patinec, V., Rolla, G. A., Botta, M., et al. (2013). Hyperfine coupling constants on inner-sphere water molecules of a triazacyclononane-based Mn(II) complex and related systems relevant as MRI contrast agents. *Inorganic Chemistry*. https://doi.org/10.1021/ic4014366

Popoola, L. T. (2019). Characterization and adsorptive behaviour of snail shell-rice husk (SS-RH) calcined particles (CPs) towards cationic dye. *Heliyon*. https://doi.org/10.1016/j.heliyon.2019.e01153

Qi, Y., Yang, M., Xu, W., et al. (2017). Natural polysaccharides-modified graphene oxide for adsorption of organic dyes from aqueous solutions. *Journal of Colloid and Interface Science, 486*, 84–96. https://doi.org/10.1016/j.jcis.2016.09.058

Ramachandran, E., & Ramukutty, S. (2014). Growth, morphology, spectral and thermal studies of gel grown diclofenac acid crystals. *Journal of Crystal Growth*. https://doi.org/10.1016/j.jcrysgro.2013.11.081

Roca Jalil, M. E., Vieira, R. S., Azevedo, D., et al. (2013). Improvement in the adsorption of thiabendazole by using aluminum pillared clays. *Applied Clay Science, 71*, 55–63. https://doi.org/10.1016/j.clay.2012.11.005

Rocha, L. S., Pereira, D., Sousa, É., Otero, M., Esteves, V. I., & Calisto, V. (2020). Recent advances on the development and application of magnetic activated carbon and char for the removal of pharmaceutical compounds from waters: A review. *Science of the Total Environment. 718*, 137272. https://doi.org/10.1016/j.scitotenv.2020.137272

Rouquerol, J., Rouquerol, F., Llewellyn, P. Maurin, G., & Sin, K.S.W. (2013). Assessment of mesoporosity. Adsorption by Powders and Porous Solids (2nd ed.), Academic Press, New York, pp 191–213.

Schwaiger, J., Ferling, H., Mallow, U., et al. (2004). Toxic effects of the non-steroidal anti-inflammatory drug diclofenac. Part I: Histopathological alterations and bioaccumulation in rainbow trout. *Aquatic Toxicology, 68*, 141–150. https://doi.org/10.1016/j.aquatox.2004.03.014

Sips, R. (1948). On the structure of a catalyst surface. *The Journal of Chemical Physics, 16*, 490–495. https://doi.org/10.1063/1.1746922

Sun, X., & Dey, S. K. (2015). Insights into the synthesis of layered double hydroxide (LDH) nanoparticles: Part 2. Formation mechanisms of LDH. *Journal of Colloid and Interface Science, 458*, 160–168. https://doi.org/10.1016/j.jcis.2015.06.025

Thommes, M., Kaneko, K., Neimark, A. V., et al. (2015). Physisorption of gases, with special reference to the evaluation of surface area and pore size distribution (IUPAC Technical Report). *Pure and Applied Chemistry*. https://doi.org/10.1515/pac-2014-1117

Triebskorn, R., Casper, H., Scheil, V., & Schwaiger, J. (2007). Ultrastructural effects of pharmaceuticals (carbamazepine, clofibric acid, metoprolol, diclofenac) in rainbow trout (Oncorhynchus mykiss) and common carp (Cyprinus carpio). *Analytical and Bioanalytical Chemistry, 387*(4), 1405–1416. https://doi.org/10.1007/s00216-006-1033-x

Vane, J. R. (1971). Inhibition of prostaglandin synthesis as a mechanism of action for aspirin-like drugs. *Nature: New Biology*. https://doi.org/10.1038/newbio231232a0

Venugopal, B. R., Shivakumara, C., & Rajamathi, M. (2007). A composite of layered double hydroxides obtained through random costacking of layers from Mg-Al and Co-Al LDHs by delamination-restacking: Thermal decomposition and reconstruction behavior. *Solid State Sciences*. https://doi.org/10.1016/j.solidstatesciences.2007.01.006

Vogna, D., Marotta, R., Napolitano, A., et al. (2004). Advanced oxidation of the pharmaceutical drug diclofenac with UV/H 2O2 and ozone. *Water Research, 38*, 414–422. https://doi.org/10.1016/j.watres.2003.09.028

Wang, Q., & Ohare, D. (2012). Recent advances in the synthesis and application of layered double hydroxide (LDH) nanosheets. *Chemical Reviews, 112*, 4124–4155.

Weber, W.J., & Morris, J.C. (1963). Kinetics of adsorption on carbon from solution. *Journal Sanitary Engineering Division, 89*(2), 31–59. https://doi.org/10.1061/JSEDAI.0000430

Wishart, D. S., Knox, C., Guo, A. C., et al. (2008). DrugBank: A knowledgebase for drugs, drug actions and drug targets. *Nucleic Acids Research*. https://doi.org/10.1093/nar/gkm958

Xiong, W., Tong, J., Yang, Z., et al. (2017). Adsorption of phosphate from aqueous solution using iron-zirconium modified activated carbon nanofiber: Performance and mechanism. *Journal of Colloid and Interface Science, 493*, 17–23. https://doi.org/10.1016/j.jcis.2017.01.024

Xu, J., Wu, L., & Chang, A. C. (2009). Degradation and adsorption of selected pharmaceuticals and personal care products (PPCPs) in agricultural soils. *Chemosphere*. https://doi.org/10.1016/j.chemosphere.2009.09.063

Yadav, S., & Dasgupta, S. (2022). Effect of time, pH, and temperature on kinetics for adsorption of methyl orange dye into the modified nitrate intercalated MgAl LDH adsorbent. *Inorganic Chemistry Communications*. https://doi.org/10.1016/j.inoche.2022.109203

Yan, Q., Gao, X., Chen, Y.-P., et al. (2014). Occurrence, fate and ecotoxicological assessment of pharmaceutically active compounds in wastewater and sludge from wastewater treatment plants in Chongqing, the Three Gorges Reservoir Area. *Science of the Total Environment, 470–471*, 618–630. https://doi.org/10.1016/j.scitotenv.2013.09.032

Yan, L. G., Yang, K., Shan, R. R., et al. (2015). Kinetic, isotherm and thermodynamic investigations of phosphate adsorption onto core-shell Fe3O4@LDHs composites with easy magnetic separation assistance. *Journal of Colloid and Interface Science*. https://doi.org/10.1016/j.jcis.2015.02.048

Yokoyama, H., & Yamatera, H. (1973). A refined Debye-Hückel theory and ion association. *Chemistry Letters*. https://doi.org/10.1246/cl.1973.337

Zhang, W., Li, H., Kan, X., et al. (2012). Adsorption of anionic dyes from aqueous solutions using chemically modified straw. *Bioresource Technology, 117*, 40–47.

Zhang, J., Wang, X., Zhan, S., Li, H., Ma, C., & Qiu, Z (2021). Synthesis of Mg/Al-LDH nanoflakes decorated magnetic mesoporous MCM-41 and its application in humic acid adsorption. *Microchemical Journal, 162*, 105839. https://doi.org/10.1016/j.microc.2020.105839

Zhao, Y., Cho, C. W., Wang, D., et al. (2020). Simultaneous scavenging of persistent pharmaceuticals with different charges by activated carbon fiber from aqueous environments. *Chemosphere, 247*, 125909. https://doi.org/10.1016/j.chemosphere.2020.125909